

Inhibition of Mitochondrial Na⁺-Ca²⁺ Exchanger Increases Mitochondrial Metabolism and Potentiates Glucose-Stimulated Insulin Secretion in Rat Pancreatic Islets

Bumsup Lee,¹ Philip D. Miles,² Leonardo Vargas,¹ Peng Luan,¹ Susan Glasco,¹ Yulia Kushnareva,¹ Elisabeth S. Kornbrust,¹ Kathryn A. Grako,¹ Claes B. Wollheim,³ Pierre Maechler,³ Jerrold M. Olefsky,² and Christen M. Anderson¹

The mitochondrial Na⁺-Ca²⁺ exchanger (mNCE) mediates efflux of Ca²⁺ from mitochondria in exchange for influx of Na⁺. We show that inhibition of the mNCE enhances mitochondrial oxidative metabolism and increases glucose-stimulated insulin secretion in rat islets and INS-1 cells. The benzothiazepine CGP37157 inhibited mNCE activity in INS-1 cells (50% inhibition at IC₅₀ = 1.5 μmol/l) and increased the glucose-induced rise in mitochondrial Ca²⁺ ([Ca²⁺]_m) 2.1 times. Cellular ATP content was increased by 13% in INS-1 cells and by 49% in rat islets by CGP37157 (1 μmol/l). Krebs cycle flux was also stimulated by CGP37157 when glucose was present. Insulin secretion was increased in a glucose-dependent manner by CGP37157 in both INS-1 cells and islets. In islets, CGP37157 increased insulin secretion dose dependently (half-maximal efficacy at EC₅₀ = 0.06 μmol/l) at 8 mmol/l glucose and shifted the glucose dose response curve to the left. In perfused islets, mNCE inhibition had no effect on insulin secretion at 2.8 mmol/l glucose but increased insulin secretion by 46% at 11 mmol/l glucose. The effects of CGP37157 could not be attributed to interactions with the plasma membrane sodium calcium exchanger, L-type calcium channels, ATP-sensitive K⁺ channels, or [Ca²⁺]_m uniporter. In hyperglycemic clamp studies of Wistar rats, CGP37157 increased plasma insulin and C-peptide levels only during the hyperglycemic phase of the study. These results illustrate the potential utility of agents that affect mitochondrial metabolism as novel insulin secretagogues. *Diabetes* 52:965–973, 2003

From the ¹Division of Metabolic Diseases, MitoKor, San Diego, California; the ²Department of Medicine, Division of Endocrinology and Metabolism, University of California, San Diego, La Jolla, California; and the ³Department of Medicine, University Medical Center, Geneva, Switzerland.

Address correspondence and reprint requests to Dr. Christen M. Anderson, Metabolic Diseases, MitoKor, 11494 Sorrento Valley Rd., San Diego, CA 92121. E-mail: andersonc@mitokor.com.

Received for publication 16 July 2002 and accepted in revised form 23 December 2002.

C.B.W., P.M., and J.M.O. have acted as consultants for MitoKor.

AUC, area under the curve; [Ca⁴⁺]_i, cytosolic calcium; [Ca²⁺]_m, mitochondrial Ca²⁺; EC₅₀, half-maximally effective concentration; FBS, fetal bovine serum; DCFC-DA, dichlorofluorescein-diacetate; GSIS, glucose-stimulated insulin secretion; IC₅₀, contraction causing 50% inhibition; K_{ATP}, ATP-sensitive K⁺; KCN, potassium cyanide; KRB, Krebs-Ringer bicarbonate; mNCE, mitochondrial Na⁺-Ca²⁺ exchanger; NCX, plasma membrane sodium-calcium exchanger; ROS, reactive oxygen species.

Mitochondrial oxidative metabolism plays an important role in the insulin secretory process in pancreatic β-cells. Stimulus-secretion coupling in the β-cell depends on the metabolism of glucose and the subsequent mitochondrial oxidative phosphorylation that generates ATP. ATP closes ATP-sensitive K⁺ (K_{ATP}) channels, causing depolarization of the β-cell membrane, opening of voltage-dependent calcium channels, and Ca²⁺ influx (1,2). Although two main processes, glycolysis and oxidative phosphorylation, are responsible for ATP synthesis during glucose metabolism, oxidative phosphorylation is the predominant pathway in the pancreatic β-cell (3,4). Insulin secretion induced by other secretagogues, such as leucine and glyceraldehydes, is also mediated by the production of ATP (5,6). The critical regulatory role of oxidative ATP production in glucose-stimulated insulin secretion (GSIS) is underscored by the observation that disrupting mitochondrial oxidative metabolism blocks nutrient-mediated insulin secretion. For example, inhibition of oxidative phosphorylation (7,8), blockade of NADH transport into mitochondria (9,10), or elimination of mitochondrial DNA from β-cells in vitro (11–15) or in vivo (16) all prevent GSIS. We tested the hypothesis that enhancing oxidative ATP production in response to glucose can increase insulin secretion. The normal feed-forward regulatory role of mitochondrial Ca²⁺ ([Ca²⁺]_m) in the β-cell was exploited to enhance oxidative metabolism.

The influx of calcium into the cytoplasm of the β-cell in response to a nutrient load triggers uptake of Ca²⁺ into the mitochondria (17–19). The resultant transient rise in [Ca²⁺]_m activates pyruvate dehydrogenase, isocitrate dehydrogenase, and α-ketoglutarate dehydrogenase, thereby stimulating oxidative phosphorylation and ATP production (20–26). In the β-cell, this pathway is proposed to act as a feed-forward mechanism for regulation of GSIS (17,27,28). Ainscow and Rutter (28) and Jouaville et al. (29) proposed that [Ca²⁺]_m also exerts a priming effect on mitochondrial ATP production, such that stimuli that increase [Ca²⁺]_m acutely have a lasting effect to enhance ATP production when oxidative substrates are provided. It may be possible to augment the [Ca²⁺]_m feed-forward and

priming mechanisms by increasing the [Ca²⁺]_m transient through inhibition of Ca²⁺ egress from the mitochondria. A major route of Ca²⁺ efflux from the mitochondria is the mitochondrial Na⁺-Ca²⁺ exchanger (mNCE) (30,31). Located in the inner mitochondrial membrane, the mNCE mediates the efflux of Ca²⁺ from mitochondria in exchange for the influx of Na⁺ (32,33). The activity of the mNCE can be rapidly and reversibly inhibited by the benzothiazepine CGP37157, a specific antagonist of the mNCE that has little effect on the activities of the voltage-dependent Ca²⁺ channel, the sarcolemmal Na⁺-Ca²⁺ exchanger, or other major mechanisms by which intact tissues regulate the cytosolic and mitochondrial Ca²⁺ levels (34,35).

We describe the use of the mNCE inhibitor CGP37157 to demonstrate that modulators of [Ca²⁺]_m in rat islets and in the INS-1 cell culture model can augment oxidative metabolism and stimulate GSIS in a glucose-dependent manner. We show that inhibition of the mNCE may represent a novel mechanism for the development of insulin secretagogues for the treatment of type 2 diabetes.

RESEARCH DESIGN AND METHODS

Isolation of rat pancreatic islets: culture of islets and INS-1 cells. Pancreatic islets from adult male Sprague Dawley (SD) rats (250–300 g; Harlan, Indianapolis, IN) were isolated using collagenase (type P; Roche Molecular Biochemicals, Indianapolis, IN) as described previously (36). All animal procedures were approved by the institutional animal care and use committee. Isolated islets were cultured for 2–7 days in CMRL-1066 medium (Sigma, St. Louis, MO) containing 5.5 mmol/l glucose, 10% fetal bovine serum (FBS), penicillin (100 units/ml), and streptomycin (100 µg/ml) at 5% CO₂-95% air at 37°C as described previously (36). INS-1 cells were maintained in RPMI-1640 medium (Mediatech, Herndon, VA) supplemented with 10% FBS, 2-mercaptoethanol (0.0004%), HEPES (10 mmol/l), pyruvate (1 mmol/l), penicillin (100 units/ml), and streptomycin (100 µg/ml) at 5% CO₂-95% air at 37°C.

mNCE assay. mNCE activity was measured in INS-1 cells that were treated with digitonin to permeabilize the plasma membrane without affecting the mitochondrial membranes. INS-1 cells in suspension were incubated with digitonin (0.007%) in sucrose buffer (250 mmol/l sucrose, 2.5 mmol/l KH₂PO₄, 10 mmol/l HEPES, pH 7.4) containing 1 µmol/l rotenone, 1 µmol/l cyclosporin A, 0.05 µmol/l calcium green, and 5 mmol/l succinate. The mitochondria were then loaded with 60 µmol/l calcium and 1 µmol/l ruthenium red. The permeabilized cell suspension was transferred to a 96-well plate in the absence or presence of CGP37157. After addition of NaCl (20 mmol/l), the rate of change in fluorescence was measured in an Fmax fluorescence plate reader, using wavelengths of 485 nm for excitation and 538 nm for emission (Molecular Devices, Sunnyvale, CA).

[Ca²⁺]_m measurement. Measurements were performed as described previously by Maechler et al. (37). Briefly, INS-1 cells that express mitochondrially targeted aequorin (INS-1/EK-3 cells) were seeded onto glass coverslips and maintained for 2–3 days in RPMI-1640 containing 10% FBS. The cells were incubated with 2.5 µmol/l coelenterazine (Calbiochem, San Diego, CA) in Krebs-Ringer bicarbonate (KRB) buffer (135 mmol/l NaCl, 3.6 mmol/l KCl, 10 mmol/l HEPES, 5 mmol/l sodium bicarbonate, 0.5 mmol/l NaH₂PO₄, 0.5 mmol/l MgCl₂, 1.5 mmol/l CaCl₂, and 0.1% BSA, pH 7.4) containing 2.8 mmol/l glucose for 2 h at 37°C before placement into a thermostatically controlled chamber for perfusion. Luminescence was measured using a photomultiplier tube/ photon-counting apparatus (model P10232; Electron Tubes, Rockaway, NJ), and [Ca²⁺]_m concentration was calculated from the luminescent readings as described previously (37).

Measurement of cytosolic calcium in INS-1 cells, single islet cells, and islets. Islets were dispersed using EDTA and trypsin as described previously (36). The imaging procedure has been described (38). Briefly, dispersed islet cells were plated onto glass coverslips and incubated at 37°C in CMRL-1066 culture medium. Cell viability as assessed by trypan blue exclusion was 95–98% for each of the islet cell groups studied. INS-1 cells, single islet cells, or islets on glass coverslips were loaded with fura-2/AM (1 µmol/l; Molecular Probes, Eugene, OR) for 20 min in KRB buffer (pH 7.4), then transferred to a closed perfusion chamber (Biopetech, Butler, PA) on an inverted microscope. Fluorescence was measured by dual-excitation fluorimetry, with excitation

and emission wavelengths set at 340/380 and 510 nm, respectively. Images were taken every 2 s for INS-1 cells and single islet cells and 20 s for islets.

For measurement of plasma membrane sodium-calcium exchanger (NCX) activity, NaCl was iso-osmotically replaced by sucrose, and NaHCO₃ was replaced by choline bicarbonate. To avoid cholinergic effects, the Na⁺-free buffer contained atropine (10 µmol/l). Cytosolic calcium ([Ca²⁺]_i) was calculated as described previously (39). KB-R7943 (Tocris, Ballwin, MO), an inhibitor of the NCX, was used as a positive control.

NAD(P)H measurement. NAD(P)H autofluorescence was measured as described by Staddon and Hansford (40). INS-1 cells were starved in glucose-free KRB buffer for 1 h at 37°C, then harvested by trypsinization. The cells were resuspended in KRB buffer, and fluorescence was measured using an excitation wavelength of 340 nm and an emission wavelength of 470 nm in a Shimadzu RF-5301PC Spectrofluorophotometer (Shimadzu, Columbia, MD). Maximal fluorescence changes were monitored after the addition of 5 µmol/l rotenone and 20 mmol/l glucose.

ATP measurement. INS-1 cells were starved for 30 min in glucose-free KRB buffer containing 1 µmol/l CGP37157 or vehicle and subsequently stimulated with various concentrations of glucose for 15 min at 37°C. For measurement of ATP in islets, islets were incubated with 15 mmol/l glucose for 30 min as described previously (41). The islets were then incubated for 30 min in glucose-free KRB buffer before addition of 1 µmol/l CGP37157 or vehicle and glucose for 30 min. ATP content was measured using Cell Titer Glo reagent (Promega, Madison, WI) according to the manufacturer's instructions.

Measurement of reactive oxygen species. For measurement of reactive oxygen species (ROS) by dichlorofluorescein-diacetate (DCF-DA) oxidation (Molecular Probes), INS-1 cells were suspended in glucose-free KRB buffer and incubated 1 h at 37°C. DCF-DA (100 µmol/l) was added to all cells; compound and glucose were added as appropriate. After 2 h at 37°C, the fluorescence was read at an excitation wavelength of 485 nm and an emission wavelength of 530 nm. For measurement by Amplex-Red oxidation, INS-1 cells were incubated for 2 h with compounds and glucose before addition of the Amplex reagent according to the manufacturer's instructions (Molecular Probes). Fluorescence was measured at an excitation wavelength of 530 nm and emission wavelength of 590 nm.

Insulin release. For static measurements, isolated islets were preincubated in oxygenated KRB buffer (pH 7.4) containing 16 mmol/l HEPES, 0.01% BSA, and 5.5 mmol/l glucose for 60 min in the absence or presence of CGP37157, followed by a 20-min treatment in fresh buffer with glucose and CGP37157. Insulin release was expressed as the difference between buffer insulin content at 20 min and at time 0. INS-1 cells were starved for 2 h in glucose-free RPMI-1640 medium containing 1% FBS before measurement of insulin secretion in the presence of glucose and CGP37157 over a 30-min period at 37°C. For islet perfusion, groups of 100 islets were preperfused for 60 min with oxygenated KRB buffer (pH 7.4) containing 2.8 mmol/l glucose, 0.1 mmol/l 3-isobutyl-1-methylxanthine, and 0.5% BSA at a rate of 0.5 ml/min. Fractions were collected every 2 min for insulin measurements by insulin enzyme-linked immunosorbent assay kit (Crystal Chem, Chicago; ALPCO, Windham, NH) using rat insulin as standards.

Pharmacokinetic evaluation of CGP37157. CGP37157 was administered intravenously at 1 mg/kg or orally at 1, 10, and 30 mg/kg to adult male SD rats (250 g; Harlan). Blood samples were collected at various times after administration. Plasma CGP37157 concentrations were measured by liquid chromatography/mass spectrometry.

Hyperglycemic clamp studies in vivo. Male Wistar rats (Charles River Laboratories, Worcester, MA), weighing 250–300 g, were housed individually under controlled light (12/12 h) and temperature conditions and given access to diet and water ad libitum. All procedures were in accordance with the Guide for the Care and Use of Laboratory Animals of the National Institutes of Health and approved by the Animal Subjects Committee of the University of California, San Diego. After a 2- to 3-day acclimation period, two catheters were placed in the right jugular vein (Micro-Renathane MRE-033, 0.033 in outer diameter and 0.014 in inner diameter; Braintree Scientific, Braintree, MA), and another was placed in the left carotid artery under general anesthesia. The anesthetic cocktail consisted of ketamine HCl (50 mg/kg) (Fort Dodge Animal Health, Fort Dodge, IA), acepromazine maleate (1 mg/kg) (Butler, Columbus, OH), and xylazine (4.8 mg/kg) (Butler) given intramuscularly. Four days after catheter placement, animals were randomly assigned to two groups. CGP37157 or vehicle (10% ethanol, 30% polyethylene glycol-400, 15% propylene glycol, and 45% water) was infused at 3.5 mg · kg⁻¹ · h⁻¹ for 5 h after a loading dose of 4.3 mg/kg. A glucose infusion (25 mg · kg⁻¹ · min⁻¹) was then begun. Blood samples (200 µl) were collected into tubes containing aprotinin (250 KIU/ml; Calbiochem) at the beginning of the experiment, before the glucose infusion, and at intervals during the glucose infusion. Blood glucose was measured using a B-Glucose Analyzer (HemoCue, Mission Viejo, CA). Plasma insulin concentrations were measured using a rat insulin

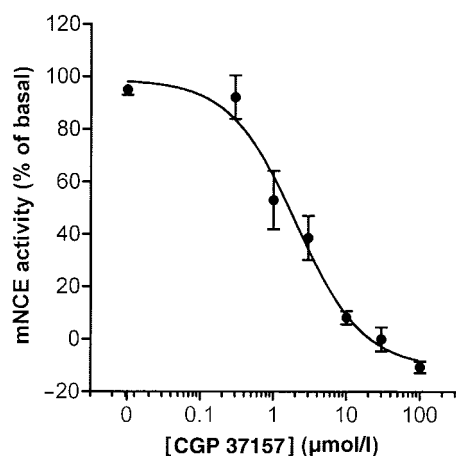


FIG. 1. CGP37157 inhibits mNCE activity in INS-1 cells. Digitonin-permeabilized cells were loaded with calcium and treated with CGP37157 or vehicle. NaCl was added to induce $[Ca^{2+}]_m$ efflux through the mNCE. Activity is expressed as the rate of change of fluorescence relative to vehicle alone. Data are means \pm SE of four experiments.

enzyme-linked immunosorbent assay. Plasma C-peptide concentrations were measured using a radioimmunoassay (Linco, St. Charles, MO).

Statistical analysis. Data are given as means \pm SE. The differences between treatment groups were analyzed by the Student's *t* test or one-way ANOVA, with post hoc analysis using the Student-Newman-Keuls multiple comparison test. For animal studies, two-way ANOVA was used. $P < 0.05$ was accepted as significant.

RESULTS

CGP37157 inhibits the mNCE in INS-1 cells. To ensure that mNCE activity was present in INS-1 cells and to characterize the sensitivity of the activity to CGP37157, a fluorescent assay was used to measure Na^+ -dependent Ca^{2+} efflux from INS-1 mitochondria. CGP37157 (0.01–100 μ mol/l) inhibited mNCE activity in digitonin-permeabilized INS-1 cells in a dose-dependent fashion (Fig. 1). Half-maximal inhibition was observed at 1.5 μ mol/l, and complete inhibition of the mNCE activity was achieved at 10 μ mol/l.

mNCE inhibition increases $[Ca^{2+}]_m$ in aequorin-transfected INS-1/EK-3 cells. The resting $[Ca^{2+}]_m$ in INS-1/EK-3 cells ranged from 100 to 200 nmol/l (Fig. 2A). Glucose stimulation of the cells elicited an immediate and transient increase in $[Ca^{2+}]_m$ (Fig. 2A), as previously described by others (17). When the cells were treated with CGP37157, the peak increase was higher and the duration longer (Fig. 2A) than in control cells, such that the area under the curve (AUC) was increased 2.1 times by the mNCE inhibitor. Glucose increased $[Ca^{2+}]_m$ in INS-1/EK-3 cells in a dose-dependent manner (Fig. 2B). The glucose dose-response curve was shifted to the left, and the maximal $[Ca^{2+}]_m$ increased slightly by CGP37157 (1 μ mol/l).

CGP37157 enhances NADH production. Acute changes in the NADH content of cells can be used as an indicator of the flux through the Krebs cycle. To determine whether inhibition of the mNCE enhanced Krebs cycle flux, NADH autofluorescence was measured in INS-1 cells under a variety of conditions. Basal autofluorescence was unchanged in INS-1 cells after the addition of glucose-free KRB buffer to the cells (Table 1). Glucose increased NADH autofluorescence in a dose-dependent manner. Preincubation of the cells with 0.1 or 1 μ mol/l CGP37157 had no

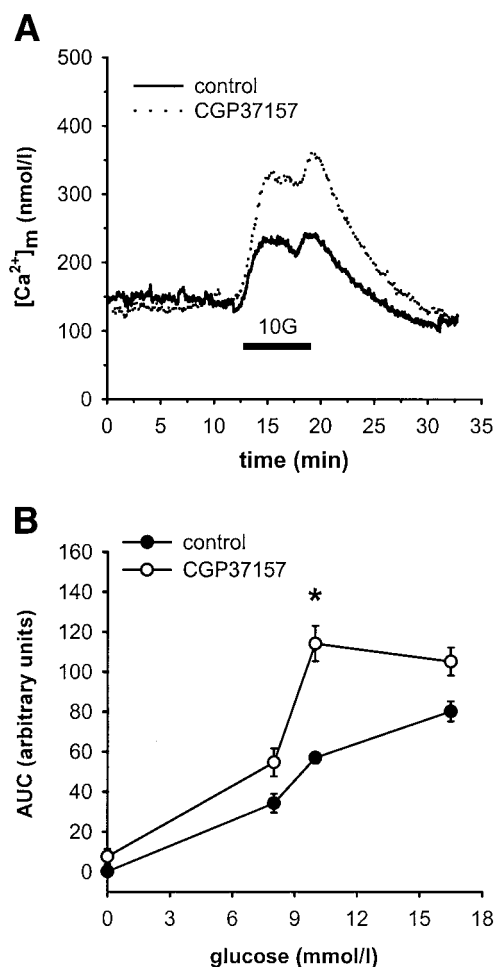


FIG. 2. Inhibition of mNCE activity enhances the glucose-induced rise in $[Ca^{2+}]_m$ in aequorin-expressing INS-1/EK-3 cells. **A:** Representative $[Ca^{2+}]_m$ recording ($n = 3$) from INS-1/EK-3 cells exposed to 10 mmol/l glucose (10 G) in the presence of 1 μ mol/l CGP37157 (dashed line) or vehicle (control, solid line). **B:** Glucose dependence of $[Ca^{2+}]_m$. Individual perfusions were performed as in A but with various glucose concentrations. Data are expressed as the AUC of the calcium tracings. Data are means \pm SE of three determinations. Differences between groups were analyzed by the Student's *t* test. * $P < 0.05$ vs. corresponding control.

effect on basal autofluorescence but enhanced the glucose-induced rise in NADH in the presence of 7 or 15 mmol/l glucose (Table 1). These observations show that CGP37157 increases Krebs cycle flux when glucose is supplied but not in the absence of oxidizable substrate.

CGP37157 increases ATP production in INS-1 cells and rat islets. CGP37157 increased the glucose-induced rise in ATP content in INS-1 cells and rat islets (Table 2).

TABLE 1
NAD(P)H autofluorescence in INS-1 cells

Glucose (mmol/l)	Change in NAD(P)H (% of maximal change)		
	Control	CGP37157 (0.1 μ mol/l)	CGP37157 (1 μ mol/l)
0	-7.6 ± 10	-1.1 ± 5.6	-5.2 ± 5.6
7	29.5 ± 3.5	38.2 ± 6.0	$42.5 \pm 3.4^*$
15	47.3 ± 3.4	$65.3 \pm 4.0^*$	$61.5 \pm 3.9^*$

Data are means \pm SE of eight measurements. Changes in NAD(P)H content were monitored in INS-1 cells during the addition of glucose after pretreatment with CGP37157 or vehicle. * $P < 0.01$ vs. control.

TABLE 2
ATP production in INS-1 cells and rat pancreatic islets

Glucose (mmol/l)	Control	CGP37157 (1 μmol/l)
INS-1 cells		
0	0.059 ± 0.008	0.063 ± 0.007
3.5	0.060 ± 0.009	0.068 ± 0.007
5.5	0.069 ± 0.004	0.078 ± 0.003*
12	0.083 ± 0.011	ND
Rat islets		
5.5	0.408 ± 0.022	0.590 ± 0.014*
8	0.578 ± 0.011	0.690 ± 0.029*
17	0.747 ± 0.005	ND

Data are means ± SE of three independent measurements in quadruplicates from INS-1 cells and in triplicates from islets. Data for INS-1 cells are in nanomoles and data for rat islets are in picomoles per islet. INS-1 cells were incubated with CGP37157 or vehicle for 15 min after a 30-min starvation. ATP was then measured as described in RESEARCH DESIGN AND METHODS. Fifteen islets were stimulated with CGP37157 for 30 min. **P* < 0.01 vs. corresponding glucose control. ND, not determined.

In INS-1 cells, glucose alone caused a concentration-dependent increase in cellular ATP content. Addition of CGP37157 augmented the rise in ATP by 13% at 3.5 and 5.5 mmol/l glucose but had no effect in the absence of glucose. Glucose also increased ATP production in rat islets in a dose-dependent manner. Addition of CGP37157 (1 μmol/l) further increased ATP production by 45% in the presence of 5.5 mmol/l glucose and 19% at 8 mmol/l glucose.

mNCE inhibition does not increase ROS production. To determine whether inhibition of the mNCE by CGP37157 increased ROS production, INS-1 cells were incubated in the presence of CGP37157 and glucose in various concentrations. In some culture dishes, antimycin was added to enhance ROS production. ROS production was unchanged by CGP37157, either when measured by Amplex-Red oxidation, which measures primarily H₂O₂ production, or by DCFC-DA oxidation, which is a more general indicator of ROS (Table 3). Antimycin-mediated ROS production was also unaffected by CGP37157.

CGP37157 stimulates insulin secretion in rat pancreatic β-cells. Inhibition of the mNCE with CGP37157 increased insulin secretion from rat islets in both static and perfusion experiments (Fig. 3). In the presence of 5.5 mmol/l glucose, CGP37157 had no significant effect on insulin secretion at concentrations <10 μmol/l. In contrast, when incubations were performed with 8 mmol/l

TABLE 3
ROS production in INS-1 cells

Glucose (mmol/l)	ROS production (% of control)			
	Control	CGP37157 (0.1 μmol/l)	CGP37157 (1 μmol/l)	CGP37157 (10 μmol/l)
DCFC-DA				
0	100 ± 6.2	101 ± 4.3	ND	103 ± 6.9
5	109 ± 9.7	97.6 ± 5.3	ND	130 ± 21
Amplex-Red				
5	100 ± 1.1	ND	89.1 ± 5.8	ND
15	92.1 ± 15	ND	88.3 ± 2.7	ND
15 + antimycin	174 ± 1.1	ND	168 ± 0.5	ND

Data are means ± SE of five to six measurements. INS-1 cells were incubated with CGP37157 or vehicle for 2 h. ROS production was then measured by DCFC-DA oxidation and by resorufin production from Amplex-Red. ND, not determined.

glucose, CGP37157 at 10 μmol/l increased GSIS to 166% of the basal level. The stimulatory effect of CGP37157 on GSIS exhibited a half-maximally effective concentration (EC₅₀) of 0.06 ± 0.02 μmol/l, and the increase was maximal at 0.1 μmol/l CGP37157 (Fig. 3A). When the CGP37157 concentration was held constant (0.1 μmol/l) and the glucose concentration varied, CGP37157 enhanced GSIS and shifted the glucose dose-response curve to the left (Fig. 3B). CGP37157 did not increase GSIS beyond the maximal effect observed with 30 mmol/l glucose. CGP37157 also enhanced insulin secretion in a dose-dependent manner in INS-1 cells (Fig. 3C). In the absence of glucose, CGP37157 at concentrations <10 μmol/l did not change insulin secretion. However, CGP37157 increased GSIS (8 mmol/l) to 156% of the control level at 0.1 μmol/l and 145% at 1 μmol/l.

In perfused rat islets, CGP37157 (0.1 μmol/l) did not change insulin secretion in basal glucose (2.8 mmol/l) but enhanced GSIS (AUC = 146% of glucose alone; *n* = 5) (Fig. 4). When islets were perfused with glucose-free buffer, CGP37157 (0.1 μmol/l) did not change insulin secretion (data not shown).

mNCE inhibition has secondary effects on [Ca²⁺]_i in islets and INS-1 cells. To determine whether CGP37157 alters [Ca²⁺]_i in pancreatic β-cells, [Ca²⁺]_i was measured in INS-1 cells and in single islet cells. CGP37157 induced an increase in [Ca²⁺]_i in the form of discrete transients and/or spikes in single islet cells (Fig. 4A; representative tracings from four experiments) and INS-1 cells (Fig. 4B). The effects of CGP37157 were reversible upon its removal from the perfusate and upon restimulation with tolbutamide (0.5 mmol/l), which increased [Ca²⁺]_i in single islet cells and in INS-1 cells (Fig. 4A and B). Pretreatment of islet cells with potassium cyanide (KCN) (100 μmol/l), an inhibitor of mitochondrial electron transport chain complex IV, abolished CGP37157-induced increases in [Ca²⁺]_i in single islet cells (Fig. 4C; representative tracing from four experiments).

CGP37157 does not affect plasma membrane Na⁺/Ca²⁺ exchange activity in islets. NCX activity was measured in intact islets by removing sodium from the external medium, forcing the exchanger to function in reverse mode to expel sodium from the cells in exchange for calcium. NCX activity, as measured by AUC during sodium removal, remained constant in untreated cells during three successive measurements (Fig. 5A). Nimodipine decreased the AUC to 76 ± 5.6% of the control value,

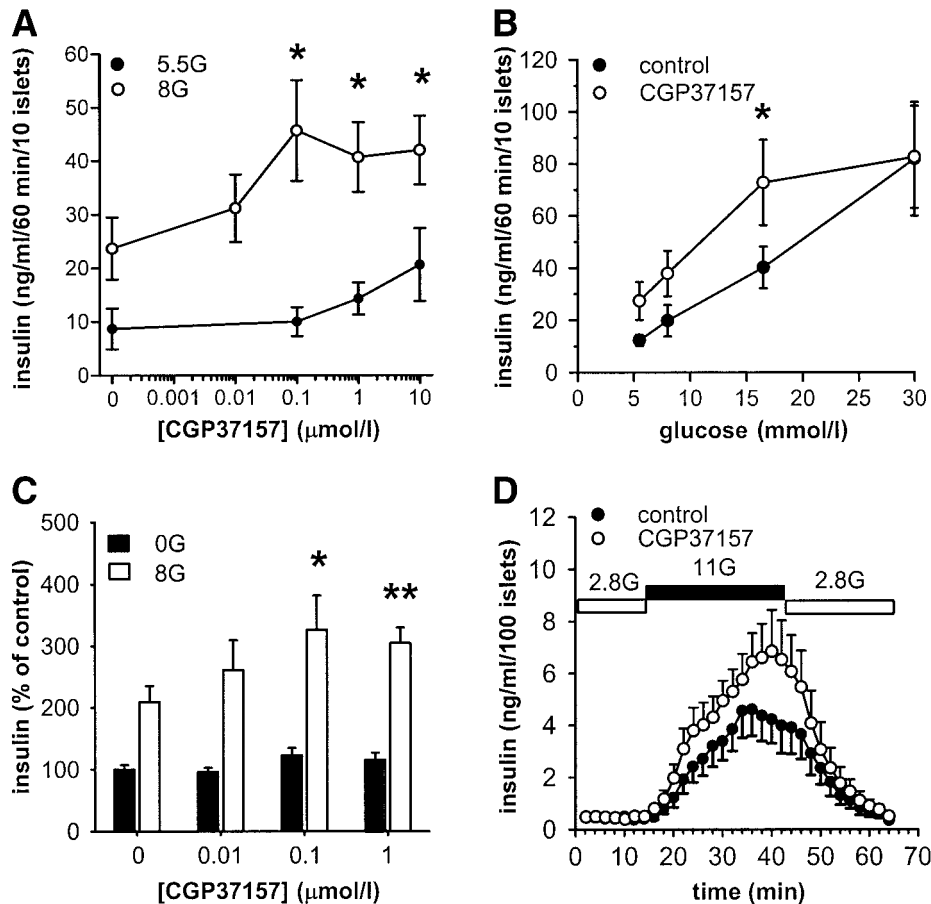


FIG. 3. mNCE inhibition enhances GSIS in rat pancreatic islets and in INS-1 cells. **A:** Insulin secretion from islets preincubated with CGP37157 (1 nmol/l to 10 μ mol/l) for 1 h, then treated with 5.5 (5G) or 8 (8G) mmol/l glucose for 20 min. * P < 0.05 vs. 8 mmol/l glucose alone (n = 5). **B:** Insulin secretion from islets preincubated with CGP37157 (0.1 μ mol/l) for 1 h before addition of various concentrations of glucose. * P < 0.05 vs. respective glucose control (n = 5). **C:** Insulin secretion from INS-1 cells preincubated with CGP37157 (0.01–1.0 μ mol/l) for 10 min before stimulation with 8 mmol/l glucose. * P < 0.05 vs. 8 mmol/l glucose alone (n = 4); ** P < 0.01 vs. 8 mmol/l glucose alone (n = 4). **D:** Islets were perfused for 1 h with 2.8 mmol/l glucose before stimulation with 11 mmol/l glucose in the presence of CGP37157 (0.1 μ mol/l) or vehicle (control). Data are means \pm SE of five experiments.

indicating that calcium uptake in this system was mediated in part by L-type calcium channels (Fig. 5B). KB-R7943, a specific inhibitor of the NCX, eliminated the residual cytosolic calcium increase (Fig. 5B). In contrast, CGP37157 had no effect on cytosolic calcium uptake compared with that in the presence of nimodipine alone (Fig. 5C; 76 ± 1.0 vs. $73 \pm 1.2\%$ of initial AUC, respectively). Hence, CGP37157 had no effect on plasma membrane NCX activity.

CGP37157 enhances insulin secretion in vivo. GSIS was measured in vivo by performing hyperglycemic clamp studies in normal Wistar rats. CGP37157 has low solubility, has a plasma half-life of 0.9 h, and is not orally bioavailable in rats (data not shown). Therefore, the compound was infused intravenously for 5 h to achieve sustained plasma concentrations of 1.6 ± 0.2 μ mol/l. After the 5-h compound infusion, glucose was infused through a second intravenous catheter at a rate ($25 \text{ mg} \cdot \text{kg}^{-1} \cdot \text{min}^{-1}$) previously determined to yield blood glucose levels of 200 mg/dl. During a 50-min glucose infusion, blood glucose levels did not differ between vehicle- and CGP37157-infused animals (Fig. 6A). Plasma insulin (Fig. 6B) and plasma C-peptide (Fig. 6C) concentrations were significantly increased by CGP37157 during the hyperglycemic portion of the experiment but were unchanged at

basal glycemia. The maximal increase in plasma insulin was observed at 25 min after the glucose infusion was begun.

DISCUSSION

We used CGP37157, an inhibitor of the mNCE, to show that increasing $[\text{Ca}^{2+}]_m$ in response to a glucose load enhances GSIS both in vitro and in vivo. In particular, CGP37157 inhibited mNCE activity in INS-1 cells, increased the glucose-induced $[\text{Ca}^{2+}]_m$ transient in INS-1 cells, and increased the glucose-induced rise in cellular ATP concentration in both INS-1 cells and rat islets. The compound also stimulated GSIS in a dose- and glucose-dependent manner in islets and in INS-1 cells. Finally, infusion of CGP37157 into normal rats increased plasma insulin and C-peptide levels during hyperglycemic clamp experiments. These observations illustrate that increasing $[\text{Ca}^{2+}]_m$ through mNCE inhibition activates flux through the Krebs cycle, thereby increasing ATP production, which in turn augments GSIS.

The coordinate rise of $[\text{Ca}^{2+}]_m$ and cellular ATP in response to glucose in cell culture models of the pancreatic β -cell has been well documented (17,19,28,37), as has the stimulatory effect of $[\text{Ca}^{2+}]_m$ on ATP production.

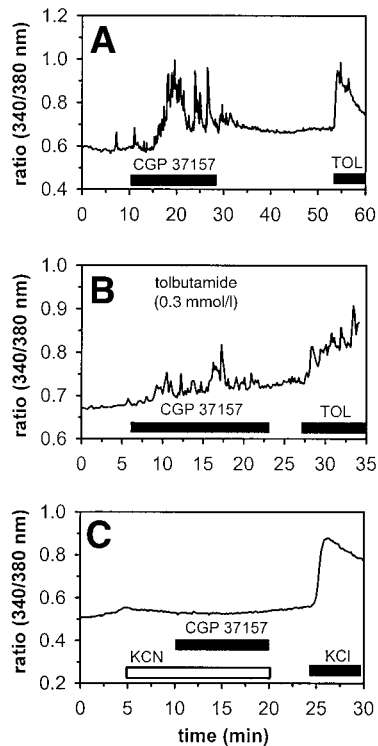


FIG. 4. CGP37157 increases $[Ca^{2+}]_i$ in single islet cells (A and C) and INS-1 cells (B). A and B: Representative tracings ($n = 4$) show changes in $[Ca^{2+}]_i$ by 1 $\mu\text{mol/l}$ CGP37157 in single islet cells and INS-1 cells, respectively. At the indicated time, CGP37157 was added. After CGP37157 was washed out, the cells were stimulated with tolbutamide (TOL; 0.5 mmol/l). C: Effect of KCN (100 $\mu\text{mol/l}$; open bar) on CGP37157-induced increases in $[Ca^{2+}]_i$ in islets. KCl (50 mmol/l) was added after CGP37157 was washed out. The glucose concentration in islet perfusions was 5.5 mmol/l.

Activation of pyruvate dehydrogenase, isocitrate dehydrogenase, and α -ketoglutarate dehydrogenase by calcium has been described in several tissues, including heart, liver, and some endocrine tissues (42–45), and occurs at $[Ca^{2+}]_m$ in the approximate range of 0.1–2.0 $\mu\text{mol/l}$ (46–48). The peak $[Ca^{2+}]_m$ achieved in the present study in glucose- and glucose plus CGP37157-treated cells was within this range, consistent with our conclusion that the elevated $[Ca^{2+}]_m$ was responsible for the enhanced Krebs cycle flux and oxidative ATP production that we observed.

The increase in $[Ca^{2+}]_m$ in the present study occurred mainly as an increase in the peak concentration, with a smaller effect on the duration of the calcium transient. Maechler et al. (37) reported that addition of CGP37157 to permeabilized INS-1 cells in the presence of succinate prolonged the $[Ca^{2+}]_m$ transient but did not increase the peak $[Ca^{2+}]_m$. The slight difference in results compared with the present study is likely due to the difference in substrate and to the use of permeabilized cells in the previous study. Using cardiac myocytes, Cox and Matlib (23) demonstrated that inhibition of the mNCE with CGP37157 increased $[Ca^{2+}]_m$ to a magnitude similar to that observed in the INS-1 cells in the present study. The increase in $[Ca^{2+}]_m$ in those studies was also associated with increased Krebs cycle flux and increased oxidative phosphorylation. We have extended the observation that mNCE inhibition increases oxidative metabolism to show that a downstream physiological consequence, namely

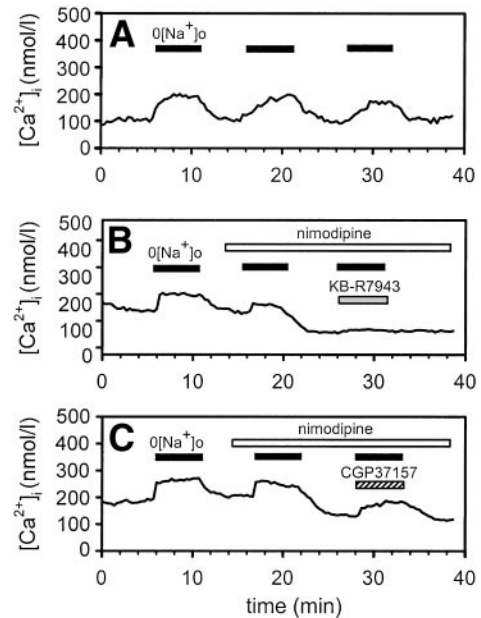


FIG. 5. Plasma membrane NCX activity in islets is not inhibited by CGP37157. A: Representative tracing ($n = 5$) showing increases in $[Ca^{2+}]_i$ induced by removing extracellular Na^+ ($0[Na^+]_o$; ■). B: Effect of KB-R7943 (10 $\mu\text{mol/l}$; ▨) on $0[Na^+]_o$ -induced changes in $[Ca^{2+}]_i$ in the presence of nimodipine (10 $\mu\text{mol/l}$; □). C: Effect of CGP37157 (1 $\mu\text{mol/l}$; ▨) on $0[Na^+]_o$ -induced changes in $[Ca^{2+}]_i$ in the presence of nimodipine (10 $\mu\text{mol/l}$; □).

GSIS, was also stimulated in islets and INS-1 cells. Although we did not measure $[Ca^{2+}]_m$ in islets in the present study, the similar increases in insulin secretion and cellular ATP in INS-1 cells and islets incubated with CGP37157 suggest that mNCE inhibition acts by increasing $[Ca^{2+}]_m$ in islets as well as in INS-1 cells.

Most of the effects of mNCE inhibition by CGP37157 in β -cells occurred only in the presence of supraphysiological glucose. Neither NADH production nor cellular ATP changed when glucose concentrations were <5.5 mmol/l. Importantly, insulin secretion was also unaffected at low glucose concentrations in INS-1 cells and in islets. During perfusion experiments, CGP37157 had no effect on insulin release at 2.8 mmol/l glucose but stimulated insulin secretion significantly at 11 mmol/l glucose. Similarly, in static incubations, CGP37157 did not affect insulin secretion from islets in the presence of 5.5 mmol/l glucose until the compound concentration was ≥ 10 $\mu\text{mol/l}$. Finally, during the 5-h intravenous infusions of CGP37157 in rats, plasma insulin levels were unaffected until hyperglycemia was induced by glucose infusion. We predicted that the secretagogue effect of CGP37157 would be glucose dependent because enhanced oxidative metabolism increases ATP production only when oxidizable substrate is available to the Krebs cycle. At glucose concentrations <5 mmol/l, little flux occurs through glucokinase, which determines the glucose concentration at which insulin secretion is initiated (49). As the glucose concentration rises above the glucokinase threshold, glycolytic metabolism of glucose produces pyruvate, providing substrate for the Krebs cycle and initiating the feed-forward regulatory cycle of $[Ca^{2+}]_m$. Hence, the small increase in $[Ca^{2+}]_m$ that was induced by CGP37157 in the absence of glucose (Fig. 2B) would not be expected to increase the Krebs cycle flux, ATP, or GSIS because insufficient oxidizable substrate was present.

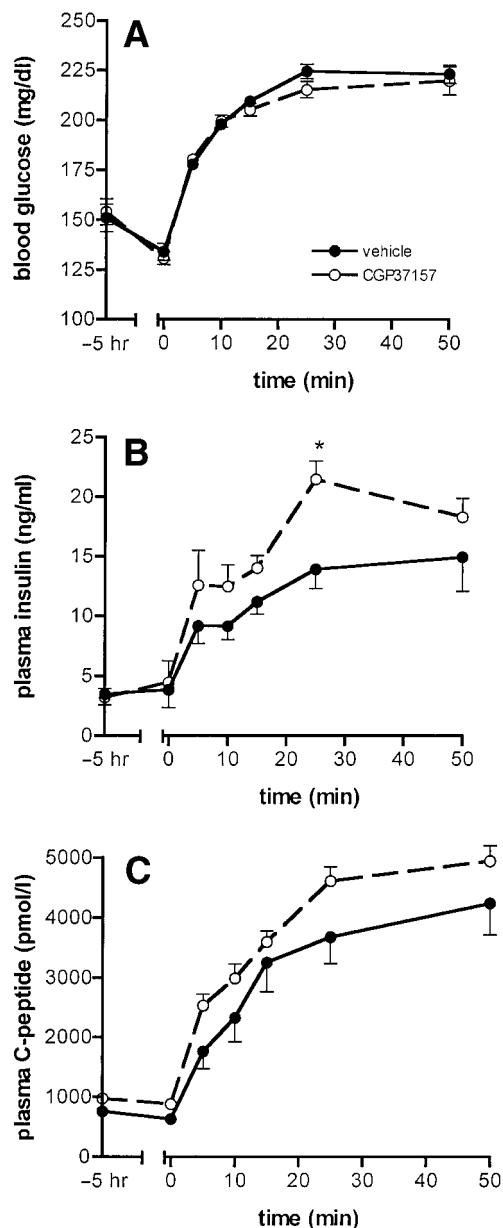


FIG. 6. Inhibition of mNCE activity increases insulin secretion during a hyperglycemic clamp in Wistar rats. CGP37157 or vehicle was infused intravenously into normal Wistar rats for 5 h. A clamped glucose infusion was then initiated to achieve a target blood glucose of 200 mg/dl. **A:** Blood glucose concentrations before and during the hyperglycemic clamp. **B:** Plasma insulin concentration: $P = 0.001$ (ANOVA); $*P < 0.01$ (Bonferroni post-test). **C:** C-peptide concentrations ($n = 6$ for each group): $P < 0.001$ (ANOVA). Data are means \pm SE of 11 vehicle-treated animals and 12 CGP37157-treated animals, except as noted.

The CGP37157-induced increases in cytosolic calcium ($[Ca^{2+}]_i$) in the present study are consistent with the proposed feed-forward mechanism of $[Ca^{2+}]_m$ in insulin secretion. That is, increased oxidative production of ATP in the presence of the mNCE inhibitor causes further depolarization of the plasma membrane and increases voltage-dependent calcium channel-mediated calcium influx into the cytoplasm. We demonstrated that, because the mitochondrial poison KCN abolished the CGP37157-mediated increase in $[Ca^{2+}]_i$, the change in $[Ca^{2+}]_i$ depended on mitochondrial oxidative metabolism (Fig. 5C).

To address the specificity of CGP37157 for the mNCE, we measured its effects on the NCX (50), an activity that is pharmacologically distinct from the mNCE. GP37157 had no measurable effect on the islet NCX, as predicted by earlier measurements that showed no effect of CGP37157 on the activity of the NCX in cardiac myocytes (35). CGP37157 had no effect on the activity of the calcium uniporter or in binding displacement assays of L-type calcium channels or K_{ATP} channels (data not shown). It is therefore unlikely that CGP37157 increased cytosolic calcium by blocking the NCX, inhibiting the calcium uniporter, blocking K_{ATP} channels, or activating L-type calcium channels.

A potential concern associated with enhancing flux through the respiratory chain is increased production of ROS, which are produced as byproducts of the electron transfer chain, primarily from complex I and ubiquinone (51). CGP37157 treatment did not increase in ROS production in INS-1 cells under conditions that enhanced oxidative metabolism, probably because compensatory metabolism of the radicals by the cellular antioxidant systems occurred. Because the β -cells, which have relatively poor antioxidant capacity compared with other tissues (52), showed no ROS accumulation, it is unlikely that other tissues would accumulate ROS during systemic administration of an mNCE inhibitor.

The tissue distribution of the mNCE and its relative contribution to $[Ca^{2+}]_m$ flux in various tissues are incompletely defined. A single report claimed to have purified the mNCE protein from cardiac tissue (53). However, neither the protein sequence nor the gene that encodes the protein has been published. Based on activity measurements, the mNCE is highly expressed in heart and muscle tissues, is in low abundance in liver (54), and is intermediate in neuronal tissue (31,55,56). However, net calcium efflux from mitochondria is determined not only by the mNCE, but by a second non-sodium-dependent exchanger as well (30,54,55). Hence, although systemic administration of an mNCE inhibitor would almost certainly have effects in tissues other than the pancreatic β -cell, the significance of those effects would depend on the relative activity of the mNCE, the activity of the non-sodium-dependent calcium egress pathway, and the possible existence of tissue-specific isoforms of the mNCE that possess different sensitivities to inhibitor compounds. Further studies are required to address nonpancreatic effects of mNCE inhibition. In addition, future studies will be required to define whether inhibition of the mNCE affects specific intracellular ATP pools (27) or alters the periodicity of calcium fluxes.

In conclusion, a novel glucose-dependent insulin secretagogue mechanism has been described. Using a prototype compound to inhibit the mNCE, we have shown that modulation of mitochondrial oxidative metabolism can favorably alter insulin secretion. The mNCE represents a novel target for type 2 diabetes drug discovery efforts.

ACKNOWLEDGMENTS

The authors thank Dr. Rosario Rizutto for helpful discussions about $[Ca^{2+}]_m$ measurement and Dr. Neil Howell for critically reading the manuscript.

REFERENCES

- Laychock SG: Glucose metabolism, second messengers and insulin secretion. *Life Sci* 47:2307–2316, 1990
- Valdeolmillos M, Nadal A, Contreras D, Soria B: The relationship between glucose-induced K_{ATP} channel closure and the rise in [Ca²⁺]_i in single mouse pancreatic beta-cells. *J Physiol* 455:173–186, 1992
- Erecinska M, Bryla J, Michalik M, Meglasson MD, Nelson D: Energy metabolism in islets of Langerhans. *Biochim Biophys Acta* 1101:273–295, 1992
- Lee B, Srinivasan M, Aalinkel R, Patel MS, Laychock SG: Mitochondrial-encoded gene regulation in rat pancreatic islets. *Metabolism* 50:200–206, 2001
- Malaisse WJ: Branched-chain amino and keto acid metabolism in pancreatic islets. *Adv Enzyme Regul* 25:203–217, 1986
- McClenaghan NH, Barnett CR, O'Harte FP, Flatt PR: Mechanisms of amino acid-induced insulin secretion from the glucose-responsive BRIN-BD11 pancreatic B-cell line. *J Endocrinol* 151:349–357, 1996
- Dukes ID, McIntyre MS, Mertz RJ, Philipson LH, Roe MW, Spencer B, Worley JF 3rd: Dependence on NADH produced during glycolysis for beta-cell glucose signaling. *J Biol Chem* 269:10979–10982, 1994
- MacDonald MJ, Fahien LA: Insulin release in pancreatic islets by a glycolytic and a Krebs cycle intermediate: contrasting patterns of glyceraldehyde phosphate and succinate. *Arch Biochem Biophys* 279:104–108, 1990
- Eto K, Suga S, Wakui M, Tsubamoto Y, Terauchi Y, Taka J, Aizawa S, Noda M, Kimura S, Kasai H, Kadowaki T: NADH shuttle system regulates K_{ATP} channel-dependent pathway and steps distal to cytosolic Ca²⁺ concentration elevation in glucose-induced insulin secretion. *J Biol Chem* 274:25386–25392, 1999
- Eto K, Tsubamoto Y, Terauchi Y, Sugiyama T, Kishimoto T, Takahashi N, Yamauchi N, Kubota N, Murayama S, Aizawa T, Akanuma Y, Aizawa S, Kasai H, Yazaki Y, Kadowaki T: Role of NADH shuttle system in glucose-induced activation of mitochondrial metabolism and insulin secretion. *Science* 283:981–985, 1999
- Inoue K, Ito S, Takai D, Soejima A, Shisa H, LePecq JB, Segal-Bendirdjian E, Kagawa Y, Hayashi JI: Isolation of mitochondrial DNA-less mouse cell lines and their application for trapping mouse synaptosomal mitochondrial DNA with deletion mutations. *J Biol Chem* 272:15510–15515, 1997
- Soejima A, Inoue K, Takai D, Kaneko M, Ishihara H, Oka Y, Hayashi JI: Mitochondrial DNA is required for regulation of glucose-stimulated insulin secretion in a mouse pancreatic beta cell line, MIN6. *J Biol Chem* 271:26194–26199, 1996
- Tsuruzoe K, Araki E, Furukawa N, Shirotani T, Matsumoto K, Kaneko K, Motoshima H, Yoshizato K, Shirakami A, Kishikawa H, Miyazaki J, Shichiri M: Creation and characterization of a mitochondrial DNA-depleted pancreatic beta-cell line: impaired insulin secretion induced by glucose, leucine, and sulfonylureas. *Diabetes* 47:621–631, 1998
- Kennedy ED, Maechler P, Wollheim CB: Effects of depletion of mitochondrial DNA in metabolism secretion coupling in INS-1 cells. *Diabetes* 47:374–380, 1998
- Hayakawa T, Noda M, Yasuda K, Yorifuji H, Taniguchi S, Miwa I, Sakura H, Terauchi Y, Hayashi J, Sharp GW, Kanazawa Y, Akanuma Y, Yazaki Y, Kadowaki T: Ethidium bromide-induced inhibition of mitochondrial gene transcription suppresses glucose-stimulated insulin release in the mouse pancreatic beta-cell line βHC9. *J Biol Chem* 273:20300–20307, 1998
- Silva JP, Kohler M, Graff C, Oldfors A, Magnuson MA, Berggren PO, Larsson NG: Impaired insulin secretion and beta-cell loss in tissue-specific knockout mice with mitochondrial diabetes. *Nat Genet* 26:336–340, 2000
- Kennedy ED, Rizzuto R, Theler JM, Pralong WF, Bastianutto C, Pozzan T, Wollheim CB: Glucose-stimulated insulin secretion correlates with changes in mitochondrial and cytosolic Ca²⁺ in aequorin-expressing INS-1 cells. *J Clin Invest* 98:2524–2538, 1996
- Rutter GA, Theler JM, Murgia M, Wollheim CB, Pozzan T, Rizzuto R: Stimulated Ca²⁺ influx raises mitochondrial free Ca²⁺ to supramicromolar levels in a pancreatic beta-cell line: possible role in glucose and agonist-induced insulin secretion. *J Biol Chem* 268:22385–22390, 1993
- Tsuboi T, Da Silva Xavier G, Holz GG, Jouaville LS, Thomas AP, Rutter GA: Glucagon-like peptide-1 mobilizes intracellular Ca²⁺ and stimulates mitochondrial ATP synthesis in pancreatic MIN6 β-cells. *Biochem J* 369:287–299, 2003
- Rutter GA: Ca²⁺-binding to citrate cycle dehydrogenases. *Int J Biochem* 22:1081–1088, 1990
- McCormack JG, Halestrap AP, Denton RM: Role of calcium ions in regulation of mammalian intramitochondrial metabolism. *Physiol Rev* 70:391–425, 1990
- Hansford RG, Tsuchiya N, Pepe S: Mitochondria in heart ischaemia and aging. *Biochem Soc Symp* 66:141–147, 1999
- Cox DA, Matlib MA: Modulation of intramitochondrial free Ca²⁺ concentration by antagonists of Na⁺-Ca²⁺ exchange. *Trends Pharmacol Sci* 14:408–413, 1993
- Hansford RG: Physiological role of mitochondrial Ca²⁺ transport. *J Bioenerg Biomembr* 26:495–508, 1994
- Hajnoczky G, Robb-Gaspers LD, Seitz MB, Thomas AP: Decoding of cytosolic calcium oscillations in the mitochondria. *Cell* 82:415–424, 1995
- Robb-Gaspers LD, Burnett P, Rutter GA, Denton RM, Rizzuto R, Thomas AP: Integrating cytosolic calcium signals into mitochondrial metabolic responses. *EMBO J* 17:4987–5000, 1998
- Kennedy HJ, Pouli AE, Ainscow EK, Jouaville LS, Rizzuto R, Rutter GA: Glucose generates sub-plasma membrane ATP microdomains in single islet β-cells. *J Biol Chem* 274:13281–13291, 1999
- Ainscow EK, Rutter GA: Mitochondrial priming modifies Ca²⁺ oscillations and insulin secretion in pancreatic islets. *Biochem J* 353:175–180, 2001
- Jouaville LS, Pinton P, Bastianutto C, Rutter GA, Rizzuto R: Regulation of mitochondrial ATP synthesis by calcium: evidence for a long-term metabolic priming. *Proc Natl Acad Sci U S A* 96:13807–13812, 1999
- Rizzuto R, Bernardi P, Pozzan T: Mitochondria as all-round players of the calcium game. *J Physiol* 529:37–47, 2000
- Bernardi P: Mitochondrial transport of cations: channels, exchangers, and permeability transition. *Physiol Rev* 79:1127–1155, 1999
- Crompton M, Capano M, Carafoli E: Respiration-dependent efflux of magnesium ions from heart mitochondria. *Biochem J* 154:735–742, 1976
- Crompton M, Heid I: The cycling of calcium, sodium, and protons across the inner membrane of cardiac mitochondria. *Eur J Biochem* 91:599–608, 1978
- Cox DA, Matlib MA: A role for the mitochondrial Na⁺-Ca²⁺ exchanger in the regulation of oxidative phosphorylation in isolated heart mitochondria. *J Biol Chem* 268:938–947, 1993
- Cox DA, Conforti L, Sperelakis N, Matlib MA: Selectivity of inhibition of Na⁺-Ca²⁺ exchange of heart mitochondria by benzothiazepine CGP-37157. *J Cardiovasc Pharmacol* 21:595–599, 1993
- Lee B, Laychock SG: Atrial natriuretic peptides affect glucose-induced Ca²⁺ responses in single islet β-cells: correlation with (Ca²⁺+Mg²⁺)-ATPase activity. *Diabetes* 46:1312–1318, 1997
- Maechler P, Kennedy ED, Pozzan T, Wollheim CB: Mitochondrial activation directly triggers the exocytosis of insulin in permeabilized pancreatic beta-cells. *EMBO J* 16:3833–3841, 1997
- Lee B, Gai W, Laychock SG: Proteasomal activation mediates down-regulation of inositol 1,4,5-trisphosphate receptor and calcium mobilization in rat pancreatic islets. *Endocrinology* 142:1744–1751, 2001
- Van Eylem F, Lebeau C, Albuquerque-Silva J, Herchuelz A: Contribution of Na/Ca exchange to Ca²⁺ outflow and entry in the rat pancreatic β-cell: studies with antisense oligonucleotides. *Diabetes* 47:1873–1880, 1998
- Staddon JM, Hansford RG: The glucagons-induced activation of pyruvate dehydrogenase in hepatocytes is diminished by 4 β-phorbol 12-myristate 13-acetate. *Biochem J* 241:729–735, 1987
- Detimary P, Dejonghe S, Ling Z, Pipeleers D, Schuit F, Henquin JC: The changes in adenine nucleotides measured in glucose-stimulated rodent islets occur in beta cells but not in alpha cells and are also observed in human islets. *J Biol Chem* 273:33905–33908, 1998
- Moreno-Sanchez R, Hogue BA, Hansford RG: Influence of NAD-linked dehydrogenase activity on flux through oxidative phosphorylation. *Biochem J* 268:421–428, 1990
- Denton RM, McCormack JG: Physiological role of Ca²⁺ transport by mitochondria (Letter). *Nature* 315:635, 1985
- Marshall SE, McCormack JG, Denton RM: Role of Ca²⁺ ions in the regulation of intramitochondrial metabolism in rat epididymal adipose tissue: evidence against a role for Ca²⁺ in the activation of pyruvate dehydrogenase by insulin. *Biochem J* 218:249–260, 1984
- Rutter GA, Burnett P, Rizzuto R, Brini M, Murgia M, Pozzan T, Tavares JM, Denton RM: Subcellular imaging of intramitochondrial Ca²⁺ with recombinant targeted aequorin: significance for the regulation of pyruvate dehydrogenase activity. *Proc Natl Acad Sci U S A* 93:5489–5494, 1996
- Hansford RG: Dehydrogenase activation by Ca²⁺ in cells and tissues. *J Bioenerg Biomembr* 23:823–854, 1991
- Rutter GA, Midgley PJ, Denton RM: Regulation of the pyruvate dehydrogenase complex by Ca²⁺ within toluene-permeabilized heart mitochondria. *Biochim Biophys Acta* 1014:263–270, 1989
- Gunter TE, Gunter KK, Sheu SS, Gavin CE: Mitochondrial calcium transport: physiological and pathological relevance. *Am J Physiol* 267:C313–C339, 1994
- Matschinsky FM, Glaser B, Magnuson MA: Pancreatic β-cell glucokinase:

- closing the gap between theoretical concepts and experimental realities. *Diabetes* 47:307–315, 1998
50. Shigekawa M, Iwamoto T: Cardiac $\text{Na}^+\text{-Ca}^{2+}$ exchange: molecular and pharmacological aspects. *Circ Res* 88:864–876, 2001
51. Dykens JA: Mitochondrial free radical production and oxidative pathophysiology: implications for neurodegenerative diseases. In *Mitochondria and Free Radicals in Neurodegenerative Disease*. Beal MF, Howell N, Bodis-Wollner I, Eds. New York, Wiley-Liss, 1997, p. 29–56
52. Lenzen S, Drinkgern J, Tiedge M: Low antioxidant enzyme gene expression in pancreatic islets compared with various other mouse tissues. *Free Radic Biol Med* 20:463–466, 1996
53. Li W, Shariat-Madar Z, Powers M, Sun X, Lane RD, Garlid KD: Reconstitution, identification, purification, and immunological characterization of the 110-kDa $\text{Na}^+\text{/Ca}^{2+}$ antiporter from beef heart mitochondria. *J Biol Chem* 267:17983–17989, 1992
54. Rizzuto R, Bernardi P, Favaron M, Azzone GF: Pathways for Ca^{2+} efflux in heart and liver mitochondria. *Biochem J* 246:271–277, 1987
55. Gunter TE, Buntinas L, Sparagna G, Eliseev R, Gunter K: Mitochondrial calcium transport: mechanisms and functions. *Cell Calcium* 28:285–296, 2000
56. Scanlon JM, Brocard JB, Stout AK, Reynolds LJ: Pharmacological investigation of mitochondrial Ca^{2+} transport in central neurons: studies with CGP-37157, an inhibitor of the mitochondrial $\text{Na}^+\text{-Ca}^{2+}$ exchanger. *Cell Calcium* 28:317–327, 2000